

Primal- and Dual-Mixed Finite Element Models for Geometrically Nonlinear Shear-Deformable Beams – A Comparative Study

Edgár BERTÓTI

*Institute of Applied Mechanics
University of Miskolc*

H-3515 Miskolc-Egyetemváros, Hungary
e-mail: edgar.bertoti@uni-miskolc.hu

The relationships between the system matrices of the displacement-based, a primal-mixed, a dual-mixed and a consistent primal-dual mixed finite element model for geometrically nonlinear shear-deformable beams are investigated. Employing Galerkin-type weak formulations with the lowest possible order, constant and linear, polynomial approximations, the tangent stiffness matrices and the load vectors of the elements are derived and compared to each other in their explicit forms. The main difference between the standard and the dual-mixed element can be characterized by a geometry-, material- and mesh-dependent constant that can serve not only as a locking indicator but also to transform the displacement-based element into a shear-locking-free dual-mixed beam element. The numerical performances of the four different elements are compared to each other through two simple model problems. The superior performance of the mixed, and especially the dual-mixed, beam elements in the nonlinear case is demonstrated, not only for the deflection, but also for the force and moment computations.

Keywords: beam, shear-deformable, geometrically nonlinear, primal-mixed, dual-mixed, finite element.

1. INTRODUCTION

The standard displacement-based finite element formulation for slender beams has long been known for its poor performance when low-order polynomial approximation for the kinematical variables is applied. The numerical over-stiffening phenomenon is usually called locking. During the last few decades, several successful strategies and formulations have been developed to overcome and eliminate the different type of locking problems, not only for beams but also for plates and shells [2, 5–7, 13, 16, 19, 23].

The main directions in formulating locking-free beam elements are (i) the reduced-selective integration technique, (ii) the use of special interpolation functions that satisfy the homogeneous equilibrium equations, (iii) the application of higher-order polynomial interpolations, and (iv) the application of mixed variational principles. These strategies are not perfectly independent of each other, as there are several cases when the elements obtained by different formulations are pointed out to be equivalent, see, e.g., [20]. Beside the Galerkin-type weak formulations, other weighted residual methods, such as least-squares finite element methods [10, 17] and isogeometric collocation methods [1, 14] have been developed for elliptic boundary value problems as well. A very profound and excellent overview on beam theories and the related finite element formulations have recently been given by [15].

Mixed formulations and models approximate both the primary and secondary variables simultaneously. Depending on the weak forms chosen for the field equations, primal-mixed and dual-mixed finite element models can be constructed [6, 20, 22]. Considering the mixed approach, a large variety of variational formulations and finite element models have been developed for modeling structural members such as beams, plates and shells [3, 7, 18, 20, 25, 26]. A comparison of the least-squares and weak-form Galerkin finite element models for standard and primal-mixed formulations of shear-deformable beams is given by [11].

The primal-mixed variational formulations and finite element models are based on the continuous displacement and discontinuous surface traction approximations and they are more popular than the dual-mixed formulations and elements relying on the continuous surface traction and discontinuous displacement approximations. It is believed and proved for some cases, however, that dual-mixed finite elements give better rates of convergence for the stress (force) variables than the primal-mixed elements [12, 24]. This property can probably be traced back to the fact, that dual-mixed elements can guarantee the continuity of the surface tractions and, thus, their local equilibrium at the element interfaces.

The traction continuity for the dual-mixed elements is usually enforced by applying the λ -multiplier technique (often called hybridization, see, e.g., [6]) and, although these multipliers are displacement-like variables, they usually correspond to non-conforming displacements. This fact makes it rather difficult to explicitly compare the primal- and dual-mixed elements and their system matrices. For beams, and one-dimensional problems in general, the explicit comparison of the element matrices of the mixed formulations is possible, however, as the λ -multipliers are the nodal displacements of the elements.

The main goal of this paper is to investigate and compare the displacement-based, a primal-mixed, a dual-mixed and a consistent primal-dual mixed formulations for nonlinear shear-deformable beams, assuming von Kármán-type geomet-

ric nonlinearity. Galerkin-type weak formulations with the lowest possible order of polynomial approximation are chosen for each case. After a brief overview of the strong and weak formulations of the beam model in Sec. 2, the derivation of the tangent stiffness matrices and the load vectors of the four different finite element models is summarized in Sec. 3. The finite element matrices, obtained by applying the computer algebra system MapleTM, are compared to each other in their explicit forms and the relationships between them are given. The numerical performance of the elements based on the four different weak formulations is compared to each other in Sec. 4 through two simple model problems. The relative errors and their asymptotic rates of convergence are investigated and compared, not only for the displacement, but also for the primarily important stress variables.

2. GEOMETRICALLY NONLINEAR BEAM MODEL

A prismatic beam of length L and cross-section area A is considered in a Cartesian xyz coordinate frame. We assume that (i) the coordinate x is measured along the axis of the beam, (ii) the xz plane is a symmetry-plane for the beam, (iii) the local coordinate axes y and z are the principal axes of the cross-sections, (iv) the material of the beam is linearly elastic and isotropic, and (v) the beam is loaded in the xz plane with coupled axial- and shear-bending deformations.

2.1. Strong forms of the governing equations

In the framework of the first-order shear-deformation beam theory applied in this paper (see, e.g., [21]), the displacement field of the 3D beam is approximated as

$$u_x(x, z) = u(x) + \phi(x)z, \quad (1)$$

$$u_z(x, z) = w(x), \quad (2)$$

where $u(x)$ and $w(x)$ are the displacements of the axis of the beam in axial and transverse directions, respectively, and $\phi(x)$ is the small rotation (i.e., $\cos \phi \approx 1$, $\sin \phi \approx \phi$) of the plane cross-section around the axis y . The non-zero strain components of the beam are

$$\varepsilon_x(x, z) = \varepsilon(x) + \kappa(x)z, \quad (3)$$

$$2\varepsilon_{xz}(x, z) = \gamma(x), \quad (4)$$

where, assuming von Kármán-type nonlinearity,

$$\varepsilon(x) = u_{,x} + \frac{1}{2}w_{,x}^2, \quad (5)$$

$$\gamma(x) = w_{,x} + \phi, \quad (6)$$

$$\kappa(x) = \phi_{,x} \quad (7)$$

are the axial strain, the transverse shear strain and the curvature, respectively (a comma followed by an index x in the subscript denotes differentiation with respect to x). Relations (5)–(7) are the nonlinear kinematic equations of the beam.

The 3D stress-strain relations for the beam are given by

$$\sigma_x(x, z) = E\varepsilon_x = E\varepsilon(x) + E\kappa(x)z, \quad (8)$$

$$\sigma_{xz}(x, z) = 2G\varepsilon_{xz} = G\gamma(x), \quad (9)$$

where E and G are the constant elasticity and shear modulus, respectively. Introducing the axial and shear forces, as well as the bending moment, as

$$N(x) = \int_A \sigma_x \, dA, \quad Q(x) = k_s \int_A \sigma_{xz} \, dA, \quad M(x) = \int_A z\sigma_x \, dA, \quad (10)$$

the stress-strain relations of the beam model are

$$N(x) = EA\varepsilon(x), \quad (11)$$

$$Q(x) = k_s GA\gamma(x), \quad (12)$$

$$M(x) = EI\kappa(x), \quad (13)$$

where k_s is the constant shear correction factor and $I = \int_A z^2 \, dA$. Note that $Q(x)$ is perpendicular to the deformed axis of the beam. The shear force perpendicular to the undeformed axis x is given by

$$V(x) = Q + w_{,x} N. \quad (14)$$

From the point of view of mixed formulations, it is an important fact that the constitutive relations (11)–(13) are invertible, i.e., the strain components can uniquely be expressed in terms of forces and moment.

The equilibrium equations of the beam model are

$$N_{,x} + f_x = 0, \tag{15}$$

$$(Q + w_{,x} N)_{,x} + f_z = 0, \tag{16}$$

$$M_{,x} - Q + m_y = 0, \tag{17}$$

where $f_x(x)$, $f_z(x)$ and $m_y(x)$ are distributed external loads. For thin beams, the moment load $m_y(x)$ is usually neglected, as we do in the subsequent analysis.

Displacement and stress boundary conditions can be prescribed for the variables u , w , ϕ and N , V , M , respectively, at both ends (at $x = 0$ and $x = L$) of the beam, by paying attention to the fact that $\{u, N\}$, $\{w, V\}$ and $\{\phi, M\}$ are work-conjugate variables.

2.2. Weak forms of the governing equations

2.2.1. Kinematic equations. The first weak forms of the kinematic equations (5)–(7) of the beam model are

$$\delta\mathcal{R}_{K_1} = \int_0^L \delta N \left(\varepsilon - u_{,x} - \frac{1}{2} w_{,x}^2 \right) dx = 0, \tag{18}$$

$$\delta\mathcal{R}_{K_2} = \int_0^L \delta Q (\gamma - w_{,x} - \phi) dx = 0, \tag{19}$$

$$\delta\mathcal{R}_{K_3} = \int_0^L \delta M (\kappa - \phi_{,x}) dx = 0, \tag{20}$$

where $\delta N(x)$, $\delta Q(x)$ and $\delta M(x)$ are arbitrary test functions (virtual forces and moment). The second weak forms of the kinematic equations are obtained from (18)–(20) by applying the divergence theorem:

$$\delta\mathcal{R}_{K_4} = \int_0^L \left[\delta N \left(\varepsilon - \frac{1}{2} w_{,x}^2 \right) + \delta N_{,x} u \right] dx - [\delta N u]_0^L = 0, \tag{21}$$

$$\delta\mathcal{R}_{K_5} = \int_0^L (\delta Q \gamma + \delta Q_{,x} w - \delta Q \phi) dx - [\delta Q w]_0^L = 0, \tag{22}$$

$$\delta\mathcal{R}_{K_6} = \int_0^L (\delta M \kappa + \delta M_{,x} \phi) dx - [\delta M \phi]_0^L = 0. \tag{23}$$

2.2.2. *Equilibrium equations.* The first weak forms of the equilibrium equations (15)–(17) are

$$\delta\mathcal{R}_{E_1} = \int_0^L \delta u (N_{,x} + f_x) dx = 0, \quad (24)$$

$$\delta\mathcal{R}_{E_2} = \int_0^L \delta w (V_{,x} + f_z) dx = 0, \quad (25)$$

$$\delta\mathcal{R}_{E_3} = \int_0^L \delta\phi (M_{,x} - Q) dx = 0, \quad (26)$$

where $\delta u(x)$, $\delta w(x)$, and $\delta\phi(x)$ are arbitrary test functions (virtual displacements and rotation). The second weak forms of the equilibrium equations are obtained from (24)–(26) by applying the divergence theorem:

$$\delta\mathcal{R}_{E_4} = \int_0^L (-\delta u_{,x} N + \delta u f_x) dx + [\delta u N]_0^L = 0, \quad (27)$$

$$\delta\mathcal{R}_{E_5} = \int_0^L (-\delta w_{,x} V + \delta w f_z) dx + [\delta w V]_0^L = 0, \quad (28)$$

$$\delta\mathcal{R}_{E_6} = \int_0^L (-\delta\phi_{,x} M - \delta\phi Q) dx + [\delta\phi M]_0^L = 0. \quad (29)$$

Depending on the selection of the above weak forms, several types of variational formulation and finite element model can be constructed. A list and the properties of possible formulations for the linear case are given in [4]. Although these formulations are theoretically equivalent, the quality of the finite element solutions can be very different, especially when the low-order approximation is used, and largely depends on whether the governing equations are being taken into account in their strong, in their first or second weak forms.

In addition to the 'classical' primal-mixed and dual-mixed formulations, there exist other possibilities, as well, to construct mixed models for the present beam problem. They can be obtained by mixing the weak forms of the governing equations in such a way that one of the kinematic equations is considered in its first weak form, the others in their second weak forms, the corresponding

equilibrium equations are taken into account in their second and first weak forms, respectively. These formulations are called *primal-dual mixed* ones. Out of the six possibilities, a consistent primal-dual mixed formulation and the related finite element model are presented in Subsec. 3.4.

3. FINITE ELEMENT MODELS

The derivation of the element tangent stiffness matrices and load vectors in their explicit forms will be presented briefly in this section, considering the displacement-based, a primal-mixed, a dual-mixed and a consistent primal-dual mixed variational formulations. The constitutive equations are taken into account in their strong forms. Bubnov–Galerkin-type approximations of the lowest possible order will be applied for each unknown field and the corresponding test functions. All the results of the symbolic computations presented in this section have been performed using the computer algebra system MapleTM.

The finite element matrices will be derived for one beam element denoted by e . The mapping between the master element $\hat{e} := \{\xi \mid -1 \leq \xi \leq 1\}$ and the actual beam element $e := \{x \mid x_1 \leq x \leq x_2\}$, with nodal coordinates $x_1 < x_2$, is given by

$$x = x(\xi) = x_1 \mathcal{H}_1(\xi) + x_2 \mathcal{H}_2(\xi), \quad (30)$$

where

$$\mathcal{H}_1(\xi) = \frac{1}{2}(1 - \xi) \quad \text{and} \quad \mathcal{H}_2(\xi) = \frac{1}{2}(1 + \xi) \quad (31)$$

are the standard linear interpolation functions. The Jacobian of the mapping (30) is $J = h/2$ with the element length $h = x_2 - x_1$.

In order to derive the element matrices, the nonlinear multivariate variational equations given in Subsec. 2.2 should be linearized. Applying the usual incremental procedure (see, e.g., [2, 21]), a general variable denoted by ${}^{t+\Delta t}\mathbf{q}(x)$ at time $t + \Delta t$ is additively decomposed as

$${}^{t+\Delta t}\mathbf{q}(x) = {}^t\mathbf{q}(x) + \mathbf{q}(x), \quad (32)$$

where ${}^t\mathbf{q}(x)$ at time t is assumed to be known and $\mathbf{q}(x)$ is its unknown increment. For notational simplicity, the increment of a quantity is denoted, according to (32), by its original symbol, without any additional sign or index.

3.1. The standard displacement-based formulation

The simplest and most popular formulation is based on the second weak forms of the equilibrium Eqs (27)–(29), and can be found in several textbooks

and papers. By inserting the constitutive Eqs (12) and (13) in (27)–(29) and taking into account the kinematic Eqs (5)–(7) in their strong forms, the linearized second weak forms of the equilibrium equations for one beam element can be written as

$$\int_{x_1}^{x_2} -\delta u_{,x} EA(u_{,x} + {}^t w_{,x} w_{,x}) dx + \delta \mathcal{F}_{E_4} = 0, \quad (33)$$

$$\int_{x_1}^{x_2} -\delta w_{,x} [k_s GA(w_{,x} + \phi) + EA {}^t w_{,x} (u_{,x} + {}^t w_{,x} w_{,x}) + {}^t N w_{,x}] dx + \delta \mathcal{F}_{E_5} = 0, \quad (34)$$

$$\int_{x_1}^{x_2} [-\delta \phi_{,x} EI \phi_{,x} - \delta \phi k_s GA(w_{,x} + \phi)] dx + \delta \mathcal{F}_{E_6} = 0, \quad (35)$$

where

$$\delta \mathcal{F}_{E_4} = \int_{x_1}^{x_2} (-\delta u_{,x} {}^t N + \delta u {}^{t+\Delta t} f_x) dx + [\delta u {}^{t+\Delta t} N]_{x_1}^{x_2}, \quad (36)$$

$$\delta \mathcal{F}_{E_5} = \int_{x_1}^{x_2} (-\delta w_{,x} {}^t V + \delta w {}^{t+\Delta t} f_z) dx + [\delta w {}^{t+\Delta t} V]_{x_1}^{x_2}, \quad (37)$$

$$\delta \mathcal{F}_{E_6} = \int_{x_1}^{x_2} (-\delta \phi_{,x} {}^t M - \delta \phi {}^t Q) dx + [\delta \phi {}^{t+\Delta t} M]_{x_1}^{x_2} \quad (38)$$

are the differences between the external virtual work at time $t + \Delta t$ and the internal virtual work at time t . In view of (5)–(7) and (11)–(14), the stress variables at time t can be computed from the known kinematic variables ${}^t u(x)$, ${}^t w(x)$ and ${}^t \phi(x)$ as

$${}^t N = EA {}^t \varepsilon = EA \left({}^t u_{,x} + \frac{1}{2} {}^t w_{,x}^2 \right), \quad (39)$$

$${}^t Q = k_s GA {}^t \gamma = k_s GA ({}^t w_{,x} + {}^t \phi), \quad (40)$$

$${}^t V = {}^t Q + {}^t w_{,x} {}^t N, \quad (41)$$

$${}^t M = EI {}^t \phi_{,x}. \quad (42)$$

The lowest possible order of C_0 -continuous approximation for the independent increments $u(x)$, $w(x)$ and $\phi(x)$ over element e is linear:

$$u[\xi(x)] = u_1 \mathcal{H}_1(\xi) + u_2 \mathcal{H}_2(\xi), \tag{43}$$

$$w[\xi(x)] = w_1 \mathcal{H}_1(\xi) + w_2 \mathcal{H}_2(\xi), \tag{44}$$

$$\phi[\xi(x)] = \phi_1 \mathcal{H}_1(\xi) + \phi_2 \mathcal{H}_2(\xi), \tag{45}$$

where $u_i = u(x_i)$, $w_i = w(x_i)$ and $\phi_i = \phi(x_i)$, $i = 1, 2$ are the nodal displacement and rotation increments. Introducing the matrix of nodal increments

$$[u]^T = [u_1 \ u_2 \ w_1 \ w_2 \ \phi_1 \ \phi_2] \tag{46}$$

and approximating the test functions $\delta u(x)$, $\delta w(x)$ and $\delta \phi(x)$ by linear functions as well, the linearized variational Eqs (33)–(35) lead to the matrix equation

$$[K^{ST}] [u] = [F^{ST}], \tag{47}$$

where

$$[K^{ST}] = [K_m^{ST}] + [K_s^{ST}] + [K_b^{ST}] \tag{48}$$

is the standard tangent stiffness matrix of the beam element, indicated by the letters ST in the superscript, with the membrane, shear and bending parts

$$[K_m^{ST}] = \frac{EA}{h} \begin{bmatrix} 1 & -1 & {}^t w_{,x} & -{}^t w_{,x} & 0 & 0 \\ -1 & 1 & -{}^t w_{,x} & {}^t w_{,x} & 0 & 0 \\ {}^t w_{,x} & -{}^t w_{,x} & {}^t \varepsilon + {}^t w_{,x}^2 & -{}^t \varepsilon - {}^t w_{,x}^2 & 0 & 0 \\ -{}^t w_{,x} & {}^t w_{,x} & -{}^t \varepsilon - {}^t w_{,x}^2 & {}^t \varepsilon + {}^t w_{,x}^2 & 0 & 0 \\ 0 & 0 & 0 & 0 & 0 & 0 \\ 0 & 0 & 0 & 0 & 0 & 0 \end{bmatrix}, \tag{49}$$

$$[K_s^{ST}] = \frac{k_s GA}{h} \begin{bmatrix} 0 & 0 & 0 & 0 & 0 & 0 \\ 0 & 0 & 0 & 0 & 0 & 0 \\ 0 & 0 & 1 & -1 & -h/2 & -h/2 \\ 0 & 0 & -1 & 1 & h/2 & h/2 \\ 0 & 0 & -h/2 & h/2 & h^2/3 & h^2/6 \\ 0 & 0 & -h/2 & h/2 & h^2/6 & h^2/3 \end{bmatrix}, \tag{50}$$

$$[\mathbf{K}_b^{\text{ST}}] = \frac{EI}{h} \begin{bmatrix} 0 & 0 & 0 & 0 & 0 & 0 \\ 0 & 0 & 0 & 0 & 0 & 0 \\ 0 & 0 & 0 & 0 & 0 & 0 \\ 0 & 0 & 0 & 0 & 0 & 0 \\ 0 & 0 & 0 & 0 & 1 & -1 \\ 0 & 0 & 0 & 0 & -1 & 1 \end{bmatrix}. \quad (51)$$

The components of the membrane tangent stiffness matrix (49) at time t can be computed from the nodal displacement values as

$${}^t\varepsilon = {}^t u_{,x} + \frac{1}{2} {}^t w_{,x}^2, \quad {}^t u_{,x} = \frac{1}{h} ({}^t u_2 - {}^t u_1), \quad {}^t w_{,x} = \frac{1}{h} ({}^t w_2 - {}^t w_1). \quad (52)$$

The components of the load vector $[\mathbf{F}^{\text{ST}}]$ of the standard element are given by

$$[\mathbf{F}^{\text{ST}}]_1 = \frac{h}{2} \int_{-1}^{+1} {}^{t+\Delta t} f_x \mathcal{H}_1(\xi) d\xi + {}^t N + {}^{t+\Delta t} \tilde{N}_1, \quad (53)$$

$$[\mathbf{F}^{\text{ST}}]_2 = \frac{h}{2} \int_{-1}^{+1} {}^{t+\Delta t} f_x \mathcal{H}_2(\xi) d\xi - {}^t N + {}^{t+\Delta t} \tilde{N}_2, \quad (54)$$

$$[\mathbf{F}^{\text{ST}}]_3 = \frac{h}{2} \int_{-1}^{+1} {}^{t+\Delta t} f_z \mathcal{H}_1(\xi) d\xi + k_s GA ({}^t w_{,x} + {}^t \bar{\phi}) + {}^t w_{,x} {}^t N + {}^{t+\Delta t} \tilde{V}_1, \quad (55)$$

$$[\mathbf{F}^{\text{ST}}]_4 = \frac{h}{2} \int_{-1}^{+1} {}^{t+\Delta t} f_z \mathcal{H}_2(\xi) d\xi - k_s GA ({}^t w_{,x} + {}^t \bar{\phi}) - {}^t w_{,x} {}^t N + {}^{t+\Delta t} \tilde{V}_2, \quad (56)$$

$$[\mathbf{F}^{\text{ST}}]_5 = \frac{k_s GA}{2} \left[{}^t w_1 - {}^t w_2 - \frac{h}{3} (2 {}^t \phi_1 + {}^t \phi_2) \right] + EI {}^t \phi_{,x} + {}^{t+\Delta t} \tilde{M}_1, \quad (57)$$

$$[\mathbf{F}^{\text{ST}}]_6 = \frac{k_s GA}{2} \left[{}^t w_1 - {}^t w_2 - \frac{h}{3} ({}^t \phi_1 + 2 {}^t \phi_2) \right] - EI {}^t \phi_{,x} + {}^{t+\Delta t} \tilde{M}_2, \quad (58)$$

where

$${}^t \phi_{,x} = \frac{1}{h} ({}^t \phi_2 - {}^t \phi_1), \quad {}^t \bar{\phi} = \frac{1}{2} ({}^t \phi_1 + {}^t \phi_2), \quad (59)$$

and ${}^{t+\Delta t} \tilde{N}_i$, ${}^{t+\Delta t} \tilde{V}_i$, ${}^{t+\Delta t} \tilde{M}_i$, $i = 1, 2$ are known external loads (forces and moments) at the nodes at time $t+\Delta t$. Equations (49)–(51) show that the coupling terms between the axial and the shear-bending deformations appear only in the membrane part of the tangent stiffness matrix. The bending and shear tangent stiffnesses are the same as those of the linear beam model. Note that this standard element with equal linear interpolations (43)–(45) for the kinematic variables exhibit only shear locking, the membrane locking is avoided [21].

3.2. Primal-mixed formulation

In the primal-mixed formulation, the equilibrium equations are considered in their second weak forms (33)–(35), just like in the standard displacement-based formulation, the kinematic equations are, however, taken into account in their first weak forms (18)–(20). This allows independent approximations for the stress variables $N(x)$, $Q(x)$ and $M(x)$. The corresponding linearized variational equations for one element are

$$\int_{x_1}^{x_2} \delta N [(EA)^{-1}N - u_{,x} - {}^t w_{,x} w_{,x}] dx + \delta \mathcal{F}_{K_1} = 0, \tag{60}$$

$$\int_{x_1}^{x_2} \delta Q [(k_s GA)^{-1}Q - w_{,x} - \phi] dx + \delta \mathcal{F}_{K_2} = 0, \tag{61}$$

$$\int_{x_1}^{x_2} \delta M [(EI)^{-1}M - \phi_{,x}] dx + \delta \mathcal{F}_{K_3} = 0, \tag{62}$$

$$\int_{x_1}^{x_2} -\delta u_{,x} N dx + \delta \mathcal{F}_{E_4} = 0, \tag{63}$$

$$\int_{x_1}^{x_2} -\delta w_{,x} (Q + {}^t w_{,x} N + {}^t N w_{,x}) dx + \delta \mathcal{F}_{E_5} = 0, \tag{64}$$

$$\int_{x_1}^{x_2} (-\delta \phi_{,x} M - \delta \phi Q) dx + \delta \mathcal{F}_{E_6} = 0, \tag{65}$$

where

$$\delta \mathcal{F}_{K_1} = \int_{x_1}^{x_2} \delta N \left({}^t \varepsilon - {}^t u_{,x} - \frac{1}{2} {}^t w_{,x}^2 \right) dx, \tag{66}$$

$$\delta \mathcal{F}_{K_2} = \int_{x_1}^{x_2} \delta Q ({}^t \gamma - {}^t w_{,x} - {}^t \phi) dx, \tag{67}$$

$$\delta \mathcal{F}_{K_3} = \int_{x_1}^{x_2} \delta M ({}^t \kappa - {}^t \phi_{,x}) dx, \tag{68}$$

and $\delta \mathcal{F}_{E_4}$, $\delta \mathcal{F}_{E_5}$, $\delta \mathcal{F}_{E_6}$ are given by Eqs (36)–(38).

As the kinematic boundary conditions are essential, the primal-mixed formulation requires C_0 -continuous approximation for the increments $u(x)$, $w(x)$ and $\phi(x)$, and their lowest possible order of approximation is linear. The dynamic boundary conditions are natural and, therefore, the lowest possible order of approximation for the increments $N(x)$, $Q(x)$ and $M(x)$ is constant:

$$u[\xi(x)] = u_1 \mathcal{H}_1(\xi) + u_2 \mathcal{H}_2(\xi), \quad N(x) = N_0, \quad (69)$$

$$w[\xi(x)] = w_1 \mathcal{H}_1(\xi) + w_2 \mathcal{H}_2(\xi), \quad Q(x) = Q_0, \quad (70)$$

$$\phi[\xi(x)] = \phi_1 \mathcal{H}_1(\xi) + \phi_2 \mathcal{H}_2(\xi), \quad M(x) = M_0, \quad (71)$$

where $u_i = u(x_i)$, $w_i = w(x_i)$, $\phi_i = \phi(x_i)$, $i = 1, 2$ are the nodal increments. By applying the Bubnov–Galerkin method and eliminating the stress increments N_0 , Q_0 , M_0 at element level, variational Eqs (60)–(65) lead to the matrix equation

$$[\mathbf{K}^{\text{PM}}] [\mathbf{u}] = [\mathbf{F}^{\text{PM}}], \quad (72)$$

where $[\mathbf{u}]$ is the matrix of the nodal unknowns defined by (46) and

$$[\mathbf{K}^{\text{PM}}] = [\mathbf{K}_m^{\text{PM}}] + [\mathbf{K}_s^{\text{PM}}] + [\mathbf{K}_b^{\text{PM}}] \quad (73)$$

is the tangent stiffness matrix of the nonlinear primal-mixed beam element, indicated by the letters PM in the superscript, with membrane, shear and bending parts:

$$[\mathbf{K}_m^{\text{PM}}] = [\mathbf{K}_m^{\text{ST}}], \quad (74)$$

$$[\mathbf{K}_s^{\text{PM}}] = \frac{k_s GA}{h} \begin{bmatrix} 0 & 0 & 0 & 0 & 0 & 0 \\ 0 & 0 & 0 & 0 & 0 & 0 \\ 0 & 0 & 1 & -1 & -h/2 & -h/2 \\ 0 & 0 & -1 & 1 & h/2 & h/2 \\ 0 & 0 & -h/2 & h/2 & \boxed{h^2/4} & \boxed{h^2/4} \\ 0 & 0 & -h/2 & h/2 & \boxed{h^2/4} & \boxed{h^2/4} \end{bmatrix}, \quad (75)$$

$$[\mathbf{K}_b^{\text{PM}}] = [\mathbf{K}_b^{\text{ST}}]. \quad (76)$$

According to (74) and (79), the membrane and bending parts of the tangent stiffness matrix of the primal-mixed element are the same as those of the standard

element, given by (49) and (51). The components of the load vector $[\mathbf{F}^{\text{PM}}]$ can be written as

$$[\mathbf{F}^{\text{PM}}]_i = [\mathbf{F}^{\text{ST}}]_i, \quad i = 1, 2, 3, 4, \quad (77)$$

$$[\mathbf{F}^{\text{PM}}]_5 = \frac{k_s GA}{2} \left({}^t w_1 - {}^t w_2 - \boxed{h \overline{{}^t \phi}} \right) + EI {}^t \phi_{,x} + {}^{t+\Delta t} \widetilde{M}_1, \quad (78)$$

$$[\mathbf{F}^{\text{PM}}]_6 = \frac{k_s GA}{2} \left({}^t w_1 - {}^t w_2 - \boxed{h \overline{{}^t \phi}} \right) - EI {}^t \phi_{,x} + {}^{t+\Delta t} \widetilde{M}_2, \quad (79)$$

where $[\mathbf{F}^{\text{ST}}]_i$, $i = 1, \dots, 4$ in (77) are the load vector components (53)–(56) of the standard element and $\overline{{}^t \phi}$ is the element average rotation at time t , defined by (59)₂.

It can be seen that only the shear part (75) of the tangent stiffness matrix and the load vector components (78) and (79) differ from those of the standard displacement element given by (50) and (53)–(58). The places of difference are indicated by frames in (75), (78) and (79). As it is well known, the rather small difference between $[\mathbf{K}_s^{\text{ST}}]$ and $[\mathbf{K}_s^{\text{PM}}]$ leads to a significant improvement in the performance of the primal-mixed element, with respect to the standard one.

3.3. Dual-mixed formulation

In the dual-mixed formulation, the equilibrium equations are taken into account in their first weak forms (24)–(26), whereas the kinematic equations are considered in their second weak forms (21)–(23). As the dynamic boundary conditions are essential in this case, C_0 -continuous approximation is required for the forces and moment. The kinematic boundary conditions are natural, which means that the displacements and the rotation can be approximated discontinuously.

The element tangent stiffness matrix and the load vector for this formulation will be derived by applying the λ -multiplier technique – a method often called hybridization [6, 22]. The key point in the derivation is that the approximations of the increments of the kinematic variables in the element domain are taken to be independent from their approximated nodal values

$$u_i = u(x_i), \quad w_i = w(x_i), \quad \phi_i = \phi(x_i), \quad i = 1, 2, \quad (80)$$

and the same applies to the corresponding test functions with nodal values δu_i , δw_i , $\delta \phi_i$, $i = 1, 2$. These latter play the role of Lagrangian multipliers ensuring

the continuity of the stress variables $N(x)$, $V(x)$ and $M(x)$ at the nodes. At time $t + \Delta t$ the Lagrangian-multiplier terms for element e can be given by

$$-\left[\delta u \text{}^{t+\Delta t}N\right]_{x_1}^{x_2} = \delta u_1 \text{}^{t+\Delta t}N_1 - \delta u_2 \text{}^{t+\Delta t}N_2 = 0, \quad (81)$$

$$-\left[\delta w \text{}^{t+\Delta t}V\right]_{x_1}^{x_2} = \delta w_1 \text{}^{t+\Delta t}V_1 - \delta w_2 \text{}^{t+\Delta t}V_2 = 0, \quad (82)$$

$$-\left[\delta \phi \text{}^{t+\Delta t}M\right]_{x_1}^{x_2} = \delta \phi_1 \text{}^{t+\Delta t}M_1 - \delta \phi_2 \text{}^{t+\Delta t}M_2 = 0. \quad (83)$$

Taking into account the above considerations, the linearized second weak forms of the kinematic Eqs (21)–(23) and the linearized first weak forms of the equilibrium Eqs (24)–(26) for one element can be written as

$$\int_{x_1}^{x_2} [\delta N(EA)^{-1}N + \delta N_{,x}u - \delta N \text{}^t w_{,x} w_{,x}] dx - [\delta Nu]_{x_1}^{x_2} + \delta \mathcal{F}_{K_4} = 0, \quad (84)$$

$$\int_{x_1}^{x_2} [\delta Q(k_s GA)^{-1}Q + \delta Q_{,x}w - \delta Q \phi] dx - [\delta Qw]_{x_1}^{x_2} + \delta \mathcal{F}_{K_5} = 0, \quad (85)$$

$$\int_{x_1}^{x_2} [\delta M(EI)^{-1}M + \delta M_{,x}\phi] dx - [\delta M\phi]_{x_1}^{x_2} + \delta \mathcal{F}_{K_6} = 0, \quad (86)$$

$$\int_{x_1}^{x_2} \delta u N_{,x} dx - [\delta u N]_{x_1}^{x_2} + \delta \mathcal{F}_{E_1} = 0, \quad (87)$$

$$\int_{x_1}^{x_2} [\delta w Q_{,x} - \delta w_{,x}(\text{}^t w_{,x}N + \text{}^t N w_{,x})] dx - [\delta w Q]_{x_1}^{x_2} + \delta \mathcal{F}_{E_2} = 0, \quad (88)$$

$$\int_{x_1}^{x_2} \delta \phi (M_{,x} - Q) dx - [\delta \phi M]_{x_1}^{x_2} + \delta \mathcal{F}_{E_3} = 0, \quad (89)$$

where

$$\delta \mathcal{F}_{K_4} = \int_{x_1}^{x_2} [\delta N(\text{}^t \varepsilon - \frac{1}{2} \text{}^t w_{,x}^2) + \delta N_{,x} \text{}^t u] dx - [\delta N \text{}^t u]_{x_1}^{x_2}, \quad (90)$$

$$\delta \mathcal{F}_{K_5} = \int_{x_1}^{x_2} (\delta Q {}^t\gamma + \delta Q_{,x} {}^t w - \delta Q {}^t\phi) dx - [\delta Q {}^t w]_{x_1}^{x_2}, \quad (91)$$

$$\delta \mathcal{F}_{K_6} = \int_{x_1}^{x_2} (\delta M {}^t\kappa + \delta M_{,x} {}^t\phi) dx - [\delta M {}^t\phi]_{x_1}^{x_2}, \quad (92)$$

$$\delta \mathcal{F}_{E_1} = \int_{x_1}^{x_2} \delta u ({}^t N_{,x} + {}^{t+\Delta t} f_x) dx - [\delta u {}^t N]_{x_1}^{x_2}, \quad (93)$$

$$\delta \mathcal{F}_{E_2} = \int_{x_1}^{x_2} \delta w ({}^t V_{,x} + {}^{t+\Delta t} f_z) dx - [\delta w {}^t V]_{x_1}^{x_2}, \quad (94)$$

$$\delta \mathcal{F}_{E_3} = \int_{x_1}^{x_2} \delta \phi ({}^t M_{,x} - {}^t Q) dx - [\delta \phi {}^t M]_{x_1}^{x_2}. \quad (95)$$

Note that the zero-valued Eqs (81)–(83) have been added to (87)–(89). The lowest possible order of approximation for the increments $u(x)$, $w(x)$ and $\phi(x)$ in the element domain is constant, and that for the increments $N(x)$, $Q(x)$ and $M(x)$ is linear:

$$u(x) = u_0, \quad N[\xi(x)] = N_1 \mathcal{H}_1(\xi) + N_2 \mathcal{H}_2(\xi), \quad (96)$$

$$w(x) = w_0, \quad Q[\xi(x)] = Q_1 \mathcal{H}_1(\xi) + Q_2 \mathcal{H}_2(\xi), \quad (97)$$

$$\phi(x) = \phi_0, \quad M[\xi(x)] = M_1 \mathcal{H}_1(\xi) + M_2 \mathcal{H}_2(\xi). \quad (98)$$

The matrices of the unknowns, the element increments u_0 , w_0 , ϕ_0 and the nodal stress increments $N_i = N(x_i)$, $Q_i = Q(x_i)$, $M_i = M(x_i)$, $i = 1, 2$, appearing in (96)–(98), are given by

$$[u^e]^T = [u_0 \ w_0 \ \phi_0], \quad [s]^T = [N_1 \ N_2 \ Q_1 \ Q_2 \ M_1 \ M_2], \quad (99)$$

and the matrix $[u]$ of the unknown nodal displacement increments (80) of the element is given by (46). As $w(x)$ is approximated by a constant function in the element domain, according to (97)₁, its derivative $w_{,x}$, of which computation is required by the weak forms (84) and (88), is obtained from the independently approximated nodal values w_1 and w_2 by $w_{,x} = h^{-1}(w_2 - w_1)$, and $\delta w_{,x}$ is computed similarly.

Using variational equations (84)–(89) and applying the Bubnov–Galerkin method, all the variables in (99) can be eliminated at the element level and, as u_i , w_i and ϕ_i , $i = 1, 2$ are the nodal displacement and rotation increments, the tangent stiffness matrix and the load vector of the dual-mixed element can be derived and compared explicitly to those of the displacement-based and primal-mixed elements. After performing all the (symbolic) computations, the following matrix equation is obtained

$$[\mathbf{K}^{\text{DM}}] [\mathbf{u}] = [\mathbf{F}^{\text{DM}}], \quad (100)$$

where

$$[\mathbf{K}^{\text{DM}}] = [\mathbf{K}_m^{\text{DM}}] + [\mathbf{K}_b^{\text{DM}}] + [\mathbf{K}_s^{\text{DM}}] \quad (101)$$

is the tangent stiffness matrix of the nonlinear dual-mixed beam element, indicated by the letters DM in the superscript. Its membrane, shear and bending parts are given by:

$$[\mathbf{K}_m^{\text{DM}}] = \frac{EA}{h} \begin{bmatrix} 1 & -1 & {}^t w_{,x} & -{}^t w_{,x} & 0 & 0 \\ -1 & 1 & -{}^t w_{,x} & {}^t w_{,x} & 0 & 0 \\ {}^t w_{,x} & -{}^t w_{,x} & {}^t \bar{\varepsilon} + {}^t w_{,x}^2 & -{}^t \bar{\varepsilon} - {}^t w_{,x}^2 & 0 & 0 \\ -{}^t w_{,x} & {}^t w_{,x} & -{}^t \bar{\varepsilon} - {}^t w_{,x}^2 & {}^t \bar{\varepsilon} + {}^t w_{,x}^2 & 0 & 0 \\ 0 & 0 & 0 & 0 & 0 & 0 \\ 0 & 0 & 0 & 0 & 0 & 0 \end{bmatrix}, \quad (102)$$

$$[\mathbf{K}_s^{\text{DM}}] = \frac{1}{C_s} [\mathbf{K}_s^{\text{PM}}], \quad (103)$$

$$[\mathbf{K}_b^{\text{DM}}] = [\mathbf{K}_b^{\text{PM}}] = [\mathbf{K}_b^{\text{ST}}], \quad (104)$$

where

$${}^t \bar{\varepsilon} = (EA)^{-1} \frac{1}{2} ({}^t N_1 + {}^t N_2) \quad (105)$$

is the average axial strain of the element at time t , computed from the nodal values of the axial force, ${}^t N_1$ and ${}^t N_2$. The constant multiplier C_s , which appears in (103) and represents the difference between the shear parts of the primal-mixed and the dual-mixed elements, is given by

$$C_s = 1 + \frac{k_s G h^2}{12 E r_g^2}, \quad \text{with} \quad \lim_{h/r_g \rightarrow 0} C_s = 1, \quad (106)$$

where $r_g = \sqrt{I/A}$ is the radius of gyration of the cross-section. It is seen from (106) that C_s depends on the element size h , the geometry of the cross-section (k_s , A , I), as well as the material of the beam (E , G). For isotropic materials, $E/G = 2(1 + \nu)$, which means that C_s depends on the material through its Poisson ratio only.

The components of the load vector of the dual-mixed element, appearing on the right-hand side of (101), are obtained as:

$$[\mathbf{F}^{\text{DM}}]_1 = \frac{h}{4} \int_{-1}^{+1} {}^{t+\Delta t} f_x \, d\xi + {}^t N + {}^{t+\Delta t} \tilde{N}_1, \quad (107)$$

$$[\mathbf{F}^{\text{DM}}]_2 = \frac{h}{4} \int_{-1}^{+1} {}^{t+\Delta t} f_x \, d\xi - {}^t N + {}^{t+\Delta t} \tilde{N}_1, \quad (108)$$

$$[\mathbf{F}^{\text{DM}}]_3 = \frac{h}{4} \int_{-1}^{+1} {}^{t+\Delta t} f_z \, d\xi + \frac{1}{C_s} k_s GA ({}^t w_{,x} + {}^t \bar{\phi}) + {}^t w_{,x} {}^t N + {}^{t+\Delta t} \tilde{V}_1, \quad (109)$$

$$[\mathbf{F}^{\text{DM}}]_4 = \frac{h}{4} \int_{-1}^{+1} {}^{t+\Delta t} f_z \, d\xi - \frac{1}{C_s} k_s GA ({}^t w_{,x} + {}^t \bar{\phi}) - {}^t w_{,x} {}^t N + {}^{t+\Delta t} \tilde{V}_2, \quad (110)$$

$$[\mathbf{F}^{\text{DM}}]_5 = \frac{1}{C_s} \left\{ \frac{k_s GA}{2} \left[{}^t w_1 - {}^t w_2 - \frac{h}{3} (2 {}^t \phi_1 + {}^t \phi_2) \right] + EI {}^t \phi_{,x} \right\} + {}^{t+\Delta t} \tilde{M}_1, \quad (111)$$

$$[\mathbf{F}^{\text{DM}}]_6 = \frac{1}{C_s} \left\{ \frac{k_s GA}{2} \left[{}^t w_1 - {}^t w_2 - \frac{h}{3} ({}^t \phi_1 + 2 {}^t \phi_2) \right] - EI {}^t \phi_{,x} \right\} + {}^{t+\Delta t} \tilde{M}_2, \quad (112)$$

where ${}^t \bar{\phi}$ is the element average rotation at time t , defined by (59)₂, whereas ${}^{t+\Delta t} \tilde{N}_i$, ${}^{t+\Delta t} \tilde{Q}_i$ and ${}^{t+\Delta t} \tilde{M}_i$, $i = 1, 2$ are known external loads at the nodes. The coupling terms between the axial and the shear-bending deformations appear, again, only in the membrane part of the tangent stiffness matrices. The bending and shear parts remain unchanged during the incremental solution procedure, i.e., the sum of the bending and shear stiffness matrices, $[\mathbf{K}_s^{\text{DM}}] + [\mathbf{K}_b^{\text{DM}}]$ gives the exact stiffness matrix of the linear dual-mixed beam element derived in [4]. Its relationship with the matrices of the standard displacement based element can be written as

$$[\mathbf{K}_s^{\text{DM}}] + [\mathbf{K}_b^{\text{DM}}] = \frac{1}{C_s} ([\mathbf{K}_s^{\text{ST}}] + [\mathbf{K}_b^{\text{ST}}]), \quad (113)$$

where C_s is given by (106). Relation (113) provides an explanation for, and a justification of, the residual bending flexibility correction concept (see, e.g., [8, 9, 26]) as well, according to the discussion given in [4].

3.4. A consistent primal-dual mixed formulation

In view of the strong forms of the kinematic equation (5), a consistent finite element approximation would require that the polynomial degree of the displacement $w(x)$ be higher by one than that of the rotation $\phi(x)$ and, in view of the equilibrium equation (17), the same applies to the bending moment $M(x)$ and shear force $Q(x)$. In this sense, the three finite element models, considered in the previous sections, are not consistent, since both $w(x)$ and $\phi(x)$, as well as $M(x)$ and $Q(x)$ are approximated by the same degree of polynomials.

A consistent approximation of the lowest possible order, i.e., constant for $\phi(x)$, $N(x)$ and $Q(x)$ and linear for $u(x)$, $w(x)$ and $M(x)$, can easily be derived for the present beam model by mixing, as already mentioned in Subsec. 2.2, the weak forms (18)–(29) of the governing equations in such a way that two out of the three kinematic equations are considered in their first weak forms, and the third one in its second weak form. The equilibrium equations should then be taken into account accordingly. Among the possible formulations of this type, a consistent primal-dual mixed weak formulation is given by the following variational equations:

$$\int_{x_1}^{x_2} \delta N [(EA)^{-1}N - u_{,x} - {}^t w_{,x} w_{,x}] dx + \delta \mathcal{F}_{K_1} = 0, \quad (114)$$

$$\int_{x_1}^{x_2} \delta Q [(k_s GA)^{-1}Q - w_{,x} - \phi] dx + \delta \mathcal{F}_{K_2} = 0, \quad (115)$$

$$\int_{x_1}^{x_2} [\delta M (EI)^{-1}M + \delta M_{,x} \phi] dx - [\delta M \phi]_{x_1}^{x_2} + \delta \mathcal{F}_{K_6} = 0, \quad (116)$$

$$\int_{x_1}^{x_2} -\delta u_{,x} N dx + \delta \mathcal{F}_{E_4} = 0, \quad (117)$$

$$\int_{x_1}^{x_2} -\delta w_{,x} (Q + {}^t w_{,x} N + {}^t N w_{,x}) dx + \delta \mathcal{F}_{E_5} = 0, \quad (118)$$

$$\int_{x_1}^{x_2} \delta\phi (M_{,x} - Q) dx - [\delta\phi M]_{x_1}^{x_2} + \delta\mathcal{F}_{E_3} = 0, \quad (119)$$

where the terms $\delta\mathcal{F}_{K_1}$, $\delta\mathcal{F}_{K_2}$, $\delta\mathcal{F}_{K_6}$ and $\delta\mathcal{F}_{E_4}$, $\delta\mathcal{F}_{E_5}$, $\delta\mathcal{F}_{E_3}$ are given by Eqs (66), (67) and (92), as well as (36), (37) and (95), respectively. Equations (114)–(119) represent special combinations of the variational equations of the primal-mixed and dual-mixed formulations in Subsec. 3.2 and 3.3. As the kinematic boundary condition for $u(x)$, $w(x)$ and the dynamic boundary condition for $M(x)$ are now essential, C_0 -continuous approximation is required for these variables. The boundary conditions for $\phi(x)$, $N(x)$ and $Q(x)$ are natural, and they can be approximated discontinuously. The lowest possible order of approximation for the unknown increments is as follows:

$$u[\xi(x)] = u_1 \mathcal{H}_1(\xi) + u_2 \mathcal{H}_2(\xi), \quad N(x) = N_0, \quad (120)$$

$$w[\xi(x)] = w_1 H_1(\xi) + w_2 \mathcal{H}_2(\xi), \quad Q(x) = Q_0, \quad (121)$$

$$M[\xi(x)] = M_1 \mathcal{H}_1(\xi) + M_2 \mathcal{H}_2(\xi), \quad \phi(x) = \phi_0. \quad (122)$$

In order to ensure the continuity of $M(x)$ at the nodes, the nodal Lagrangian multipliers $\delta\phi_1$ and $\delta\phi_2$ will be introduced for element e . The corresponding variational equation is given by (83) and is already included in (119). The approximations in (120)–(122) are consistent with the strong form of the kinematic equation (6) and the equilibrium equation (17) in the sense that the polynomial degree of $w(x)$ is higher by one than $\phi(x)$, and the same applies to $M(x)$ and $Q(x)$.

The element tangent stiffness matrix for the present formulation can be obtained by eliminating the unknown increments ϕ_0 , N_0 , Q_0 and M_1 , M_2 . The final matrix equation, obtained for the nodal increments $[u]^T = [u_1 \ u_2 \ w_1 \ w_2 \ \phi_1 \ \phi_2]$, can be written as

$$([\mathbf{K}_m^{\text{PM}}] + [\mathbf{K}_s^{\text{DM}}] + [\mathbf{K}_b^{\text{DM}}]) [u] = [\mathbf{F}^{\text{ST}}], \quad (123)$$

where, according to the indices in the superscripts, the element tangent stiffness matrix is the sum of the primal-mixed membrane stiffness, (74), and the dual-mixed shear and bending stiffnesses, (103) and (104), respectively. The element load vector is equivalent to that of the displacement-based element given by (53)–(58). Taking into account the relations (74) and (113), matrix equation (123) can be written in terms of the standard element matrices alone:

$$\left\{ [\mathbf{K}_m^{\text{ST}}] + \frac{1}{C_s} ([\mathbf{K}_s^{\text{ST}}] + [\mathbf{K}_b^{\text{ST}}]) \right\} [u] = [\mathbf{F}^{\text{ST}}]. \quad (124)$$

This result indicates that using the geometry-, material- and mesh-dependent multiplier C_s defined in (106), the standard beam element can be transformed into a consistent, shear locking-free mixed element. The multiplier $1 \leq C_s < \infty$ can also be considered as a reliable shear locking indicator [4]: the higher the value of C_s , the more serious the shear locking is. An absolutely locking-free behavior of the standard beam element would belong to $C_s = 1$, it could, however, be attained only when the length h of the element is zero (for a given cross-section), or when the cross-section's radius of gyration r_g is infinity (for fixed h).

4. NUMERICAL COMPARISONS

The results and comparisons for the finite element matrices presented in Sec. 3 are supplemented here by numerical results. The solutions for two model problems will be investigated and compared: a pinned-pinned and a clamped-clamped beam subjected to uniform transverse load $f_z(x) := f_0$ (see Fig. 1). The beam of length L has a rectangular cross-section with thickness d in the z -direction and unit thickness in the y -direction. The material parameters are taken to be the same as used by several papers and textbooks, see, e.g., [21]: $E = 3 \cdot 10^7$ psi, $\nu = 0.25$; $k_s = 5/6$. Only half the length of the beam is discretized with symmetry conditions prescribed at $x = L/2$. The nonlinear finite element solutions have been obtained using a research code written in MapleTM and applying the Newton–Raphson iteration procedure. The code is based on the explicit forms of the tangent stiffness matrices and load vectors derived in Sec. 3.

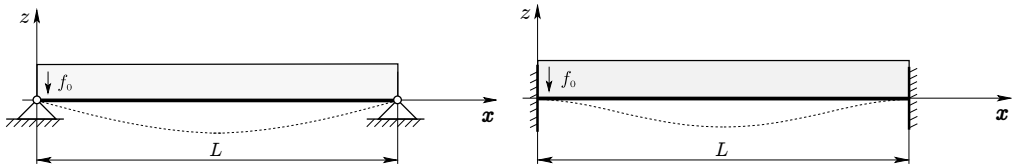


FIG. 1. Pinned-pinned and clamped-clamped beam with uniform load.

As no analytical solutions exist for the examples considered, high precision reference solutions with eight significant digits have been computed first by employing a very fine mesh of $n_e = 2^{13} = 8192$ dual-mixed elements with error tolerance $1.0e-12$ for the Euclidean norms of both the nodal displacements and the residuals. These results, used for numerical comparisons, are summarized in Tables 1 and 2 for the pinned-pinned beam and in Tables 3 and 4 for the clamped-clamped beam.

In both cases, the central deflections, the axial and shear forces as well as the bending moments are computed and listed (in absolute values) for beams with slenderness ratios $L/d = 100$ and $L/d = 1000$. Note that results and comparisons

TABLE 1. Reference solutions for the pinned-pinned beam with $L/d = 100$.

Load	w_{\max}	$N(x = L/2)$	$Q(x = 0)$	$M(x = L/2)$
1.0	3.6849610e-01	1.0159354e+03	3.7941239e+01	8.7563176e+02
2.0	5.4540671e-01	2.2324695e+03	6.0499699e+01	1.2823961e+03
3.0	6.6394944e-01	3.3167713e+03	7.8143838e+01	1.5478316e+03
4.0	7.5548870e-01	4.3036046e+03	9.3390112e+01	1.7486754e+03
5.0	8.3118727e-01	5.2189471e+03	1.0715648e+02	1.9120776e+03
6.0	8.9634624e-01	6.0792915e+03	1.1989037e+02	2.0508499e+03
7.0	9.5392496e-01	6.8956178e+03	1.3184822e+02	2.1720981e+03
8.0	1.0057557e+00	7.6756295e+03	1.4319307e+02	2.2801922e+03
9.0	1.0530575e+00	8.4249708e+03	1.5403625e+02	2.3780212e+03
10.0	1.0966861e+00	9.1479240e+03	1.6445790e+02	2.4675989e+03

TABLE 2. Reference solutions for the pinned-pinned beam with $L/d = 1000$.

Load	w_{\max}	$N(x = L/2)$	$Q(x = 0)$	$M(x = L/2)$
1.0	1.1603185e+00	1.0752867e+03	1.5239716e+00	2.3249613e+00
2.0	1.4619589e+00	1.7080321e+03	2.4176063e+00	2.9273455e+00
3.0	1.6735441e+00	2.2387518e+03	3.1667115e+00	3.3500810e+00
4.0	1.8419841e+00	2.7124628e+03	3.8350168e+00	3.6866865e+00
5.0	1.9842240e+00	3.1478448e+03	4.4489730e+00	3.9709709e+00
6.0	2.1085574e+00	3.5549331e+03	5.0227936e+00	4.2194887e+00
7.0	2.2197381e+00	3.9399055e+03	5.5652298e+00	4.4417309e+00
8.0	2.3207743e+00	4.3069057e+03	6.0821528e+00	4.6437051e+00
9.0	2.4137049e+00	4.6588838e+03	6.5777430e+00	4.8294830e+00
10.0	2.4999827e+00	4.9980339e+03	7.0551106e+00	5.0019669e+00

TABLE 3. Reference solutions for the clamped-clamped beam with $L/d = 100$.

Load	w_{\max}	$N(x = L/2)$	$Q(x = 0)$	$M(x = 0)$	$M(x = L/2)$
1.0	1.0348084e-01	7.8299930e+01	4.9999529e+01	8.2900906e+02	4.1288839e+02
2.0	2.0250814e-01	2.9986576e+02	9.9996404e+01	1.6342240e+03	8.0505072e+02
3.0	2.9424574e-01	6.3309357e+02	1.4998865e+02	2.4003218e+03	1.1633931e+03
4.0	3.7776371e-01	1.0435246e+03	1.9997516e+02	3.1220040e+03	1.4837903e+03
5.0	4.5337595e-01	1.5031599e+03	2.4995546e+02	3.8005729e+03	1.7679305e+03
6.0	5.2192918e-01	1.9922748e+03	2.9992945e+02	4.4402230e+03	2.0199507e+03
7.0	5.8438256e-01	2.4978704e+03	3.4989722e+02	5.0458275e+03	2.2444606e+03
8.0	6.4162628e-01	3.0116157e+03	3.9985892e+02	5.6219673e+03	2.4457010e+03
9.0	6.9442570e-01	3.5282232e+03	4.4981472e+02	6.1726183e+03	2.6272929e+03
10.0	7.4341852e-01	4.0443493e+03	4.9976481e+02	6.7011211e+03	2.7922347e+03

TABLE 4. Reference solutions for the clamped-clamped beam with $L/d = 1000$.

Load	w_{\max}	$N(x = L/2)$	$Q(x = 0)$	$M(x = 0)$	$M(x = L/2)$
1.0	1.1417035e+00	1.0265467e+03	4.9854277e+01	7.5552613e+01	2.4353494e+00
2.0	1.4435657e+00	1.6465343e+03	9.9595073e+01	1.2008284e+02	3.0366814e+00
3.0	1.6552632e+00	2.1683013e+03	1.4926048e+02	1.5743162e+02	3.4589289e+00
4.0	1.8237774e+00	2.6348845e+03	1.9886378e+02	1.9076187e+02	3.7952327e+00
5.0	1.9660725e+00	3.0642476e+03	2.4841263e+02	2.2138764e+02	4.0793048e+00
6.0	2.0904500e+00	3.4660752e+03	2.9791221e+02	2.5001546e+02	4.3276615e+00
7.0	2.2016674e+00	3.8463438e+03	3.4736635e+02	2.7708050e+02	4.5497753e+00
8.0	2.3027352e+00	4.2090699e+03	3.9677801e+02	3.0287484e+02	4.7516436e+00
9.0	2.3956935e+00	4.5571172e+03	4.4614958e+02	3.2760649e+02	4.9373318e+00
10.0	2.4819961e+00	4.8926184e+03	4.9548317e+02	3.5143021e+02	5.1097383e+00

for the force and moment variables are very rare in the literature, despite the fact that accurate computation of the stress variables has primary importance in the design process of structural members and, also, in the convergence of the nonlinear solution.

The convergence of the relative errors of the numerical solutions with an increasing number of elements, presented and compared subsequently to the reference solutions, has been obtained by the four formulations discussed in Sec. 3, employing uniform mesh refinement. The results and their relative errors are compared at the end of the final load step $f_0 = 10$. The reference values for that load step are listed in the last rows of Tables 1–4. Since each type of elements

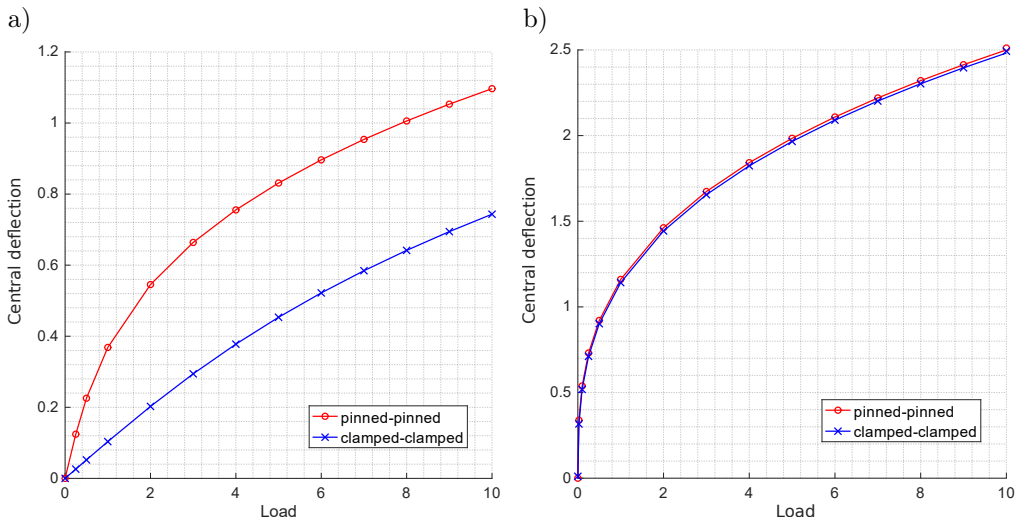


FIG. 2. Reference solution: the central deflection versus load for pinned-pinned and clamped-clamped beams with $L/d = 100$ (a) and $L/d = 1000$ (b).

has the same six degrees of freedom, according to (46), the convergence curves of the relative errors are plotted with respect to the number of elements. The total number of degrees of freedom of a mesh with n_e beam elements is $3(n_e + 1)$.

The reference solutions for the central deflection versus load are plotted in Fig. 2. The convergence of the relative error in the maximum deflection at $L/2$ is shown in Figs 3 and 4. The asymptotic rate of convergence of the relative error in the displacements is of order two for all the four elements investigated. The over-

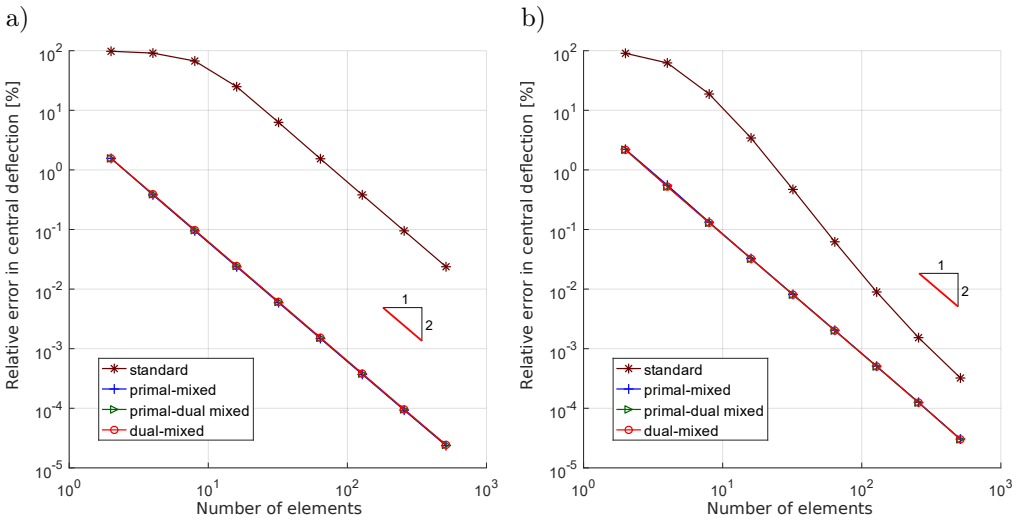


FIG. 3. Convergence of the relative error in central deflection for the pinned-pinned beam with $L/d = 100$ (a) and $L/d = 1000$ (b) at the final load step $f_0 = 10$.

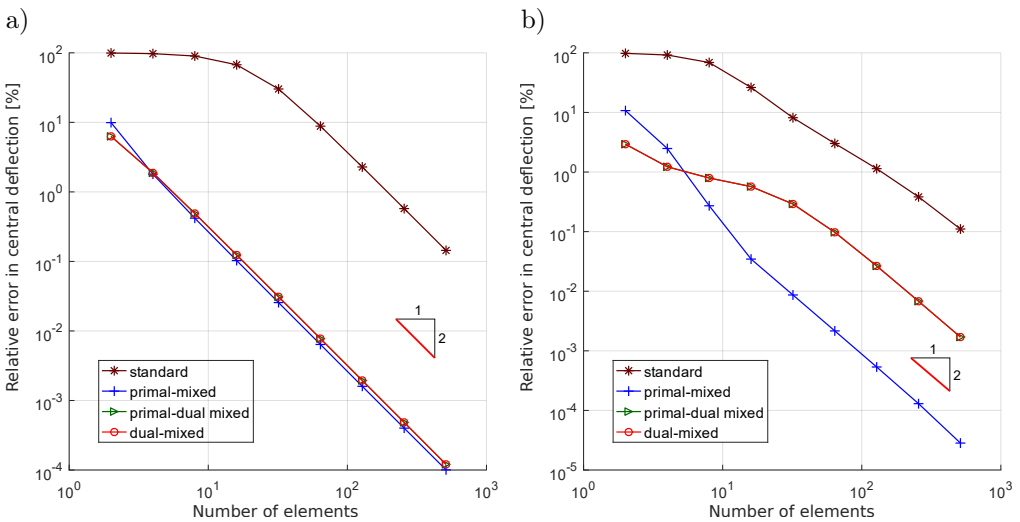


FIG. 4. Convergence of the relative error in central deflection for the clamped-clamped beam with $L/d = 100$ (a) and $L/d = 1000$ (b) at the final load step $f_0 = 10$.

stiffening behavior of the standard beam element is clearly seen from the figures. The mixed elements are not sensitive to the L/d ratio for the pinned-pinned beam. The primal-mixed element seems to be the best choice for the displacement computation.

The reference solutions for the central axial force versus load are plotted in Fig. 5. The convergence of the relative error in the axial force at $L/2$ is shown in Figs 6 and 7. The asymptotic rate of convergence of the relative error in

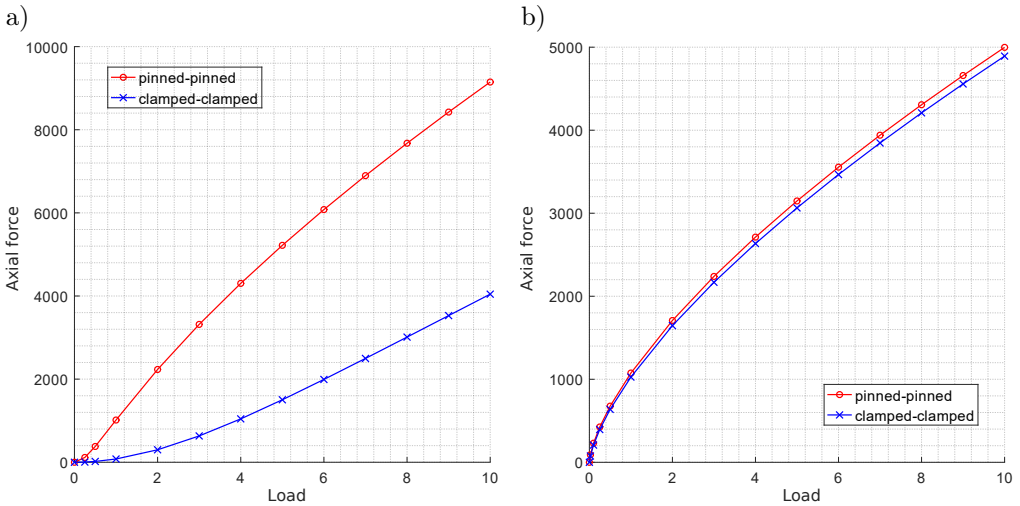


FIG. 5. Reference solution: axial force versus load at $L/2$ for pinned-pinned and clamped-clamped beams with $L/d = 100$ (a) and $L/d = 1000$ (b).

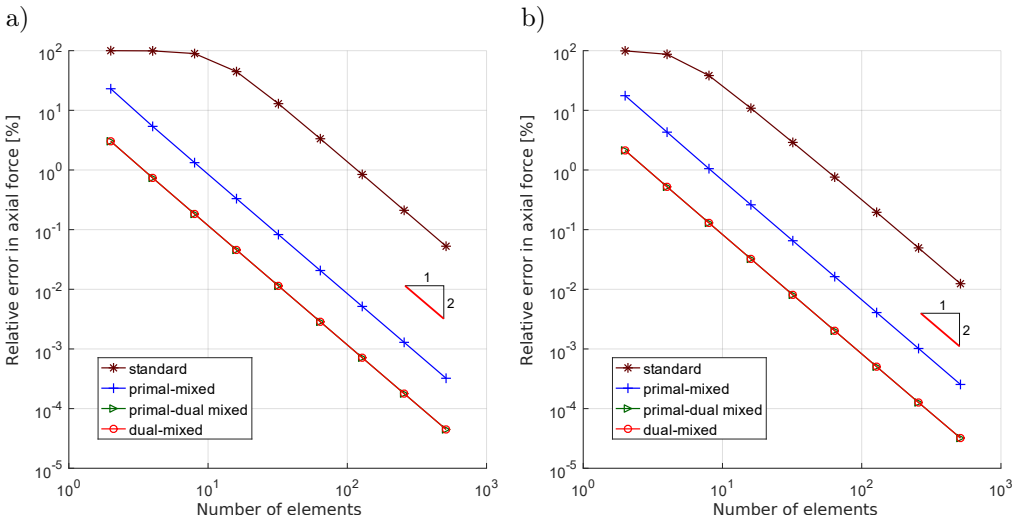


FIG. 6. Convergence of the relative error in axial force at $x = L/2$ for the pinned-pinned beam with $L/d = 100$ (a) and $L/d = 1000$ (b) at the final load step $f_0 = 10$.

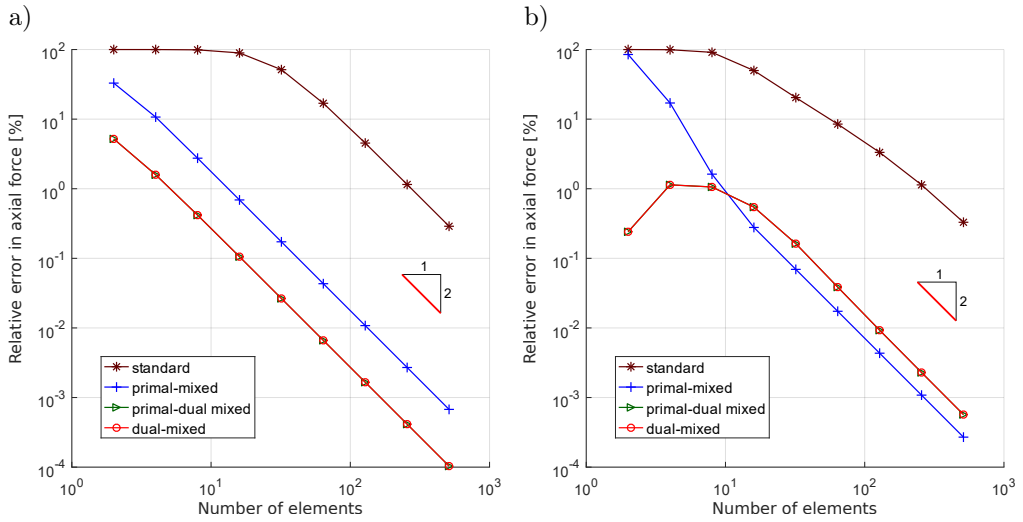


FIG. 7. Convergence of the relative error in axial force at $x = L/2$ for the clamped-clamped beam with $L/d = 100$ (a) and $L/d = 1000$ (b) at the final load step $f_0 = 10$.

the axial force is order of two, again, for each element investigated. The over-stiffening behavior of the standard beam element is clearly seen from the figures. The dual-mixed and the primal-dual mixed elements perform equivalently in this case, they seem to be the best choice for the axial force computation.

The reference solutions for the shear force Q (perpendicular to the deformed axis of the beam) versus load at $x = 0$ are plotted in Fig. 8. The conver-

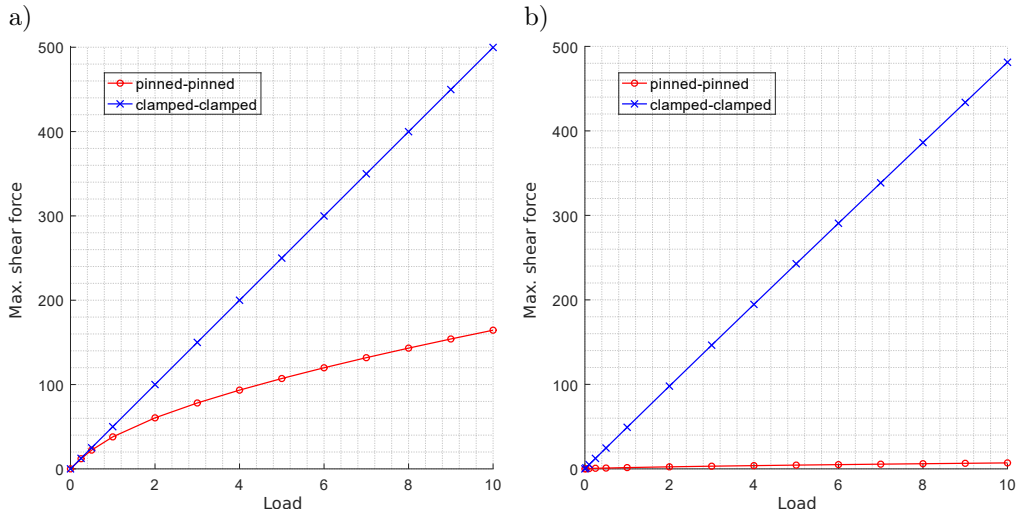


FIG. 8. Reference solution: shear force Q versus load at $x = 0$ for pinned-pinned and clamped-clamped beams with $L/d = 100$ (a) and $L/d = 1000$ (b).

gences of the relative error in the shear force Q at $x = 0$ are shown in Figs 9 and 10. The asymptotic rates of convergences depend on the boundary conditions. For the pinned-pinned beam, the standard and the dual-mixed element has second-order rates of convergence, the primal-mixed and the primal-dual mixed elements lead to first-order rates of convergence, equivalently. For clamped-clamped beam, all of the elements investigated give only first-order rates of convergence in the shear force computation. Even though the dual-

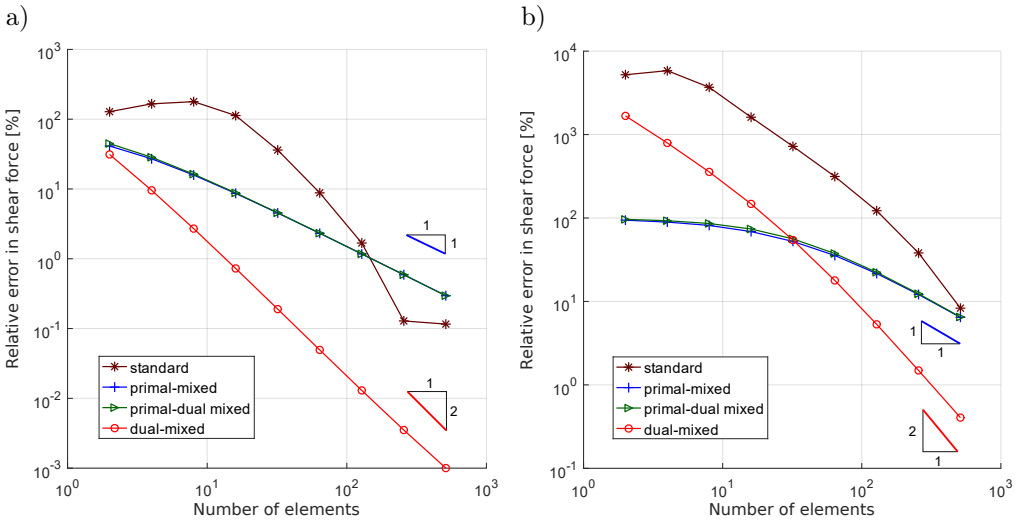


FIG. 9. Convergence of the relative error in shear force Q at $x = 0$ for the pinned-pinned beam with $L/d = 100$ (a) and $L/d = 1000$ (b) at the final load step $f_0 = 10$.

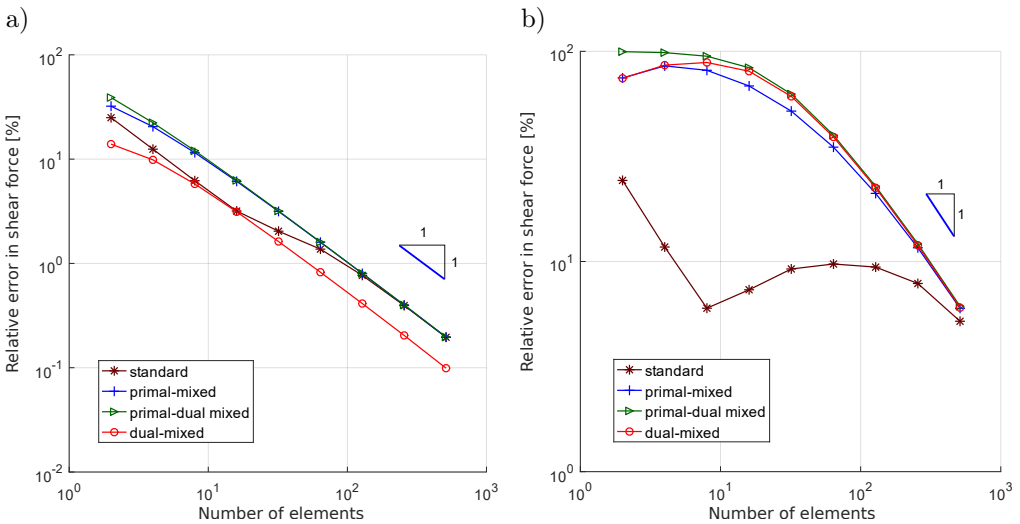


FIG. 10. Convergence of the relative error in shear force Q at $x = 0$ for the clamped-clamped beam with $L/d = 100$ (a) and $L/d = 1000$ (b) at the final load step $f_0 = 10$.

mixed element behaves rather stiff for $L/d = 1000$ with a pinned-pinned boundary condition for smaller number of elements, it appears to be the best choice for the shear force computation.

The reference solutions for the central bending moment versus load are plotted in Fig. 11. Figures 12 and 13 show the convergence curves of the relative error in the bending moment at $x = L/2$. The dual-mixed and the primal-dual mixed elements are equivalent in this case, they give a second-order rate of asymptotic

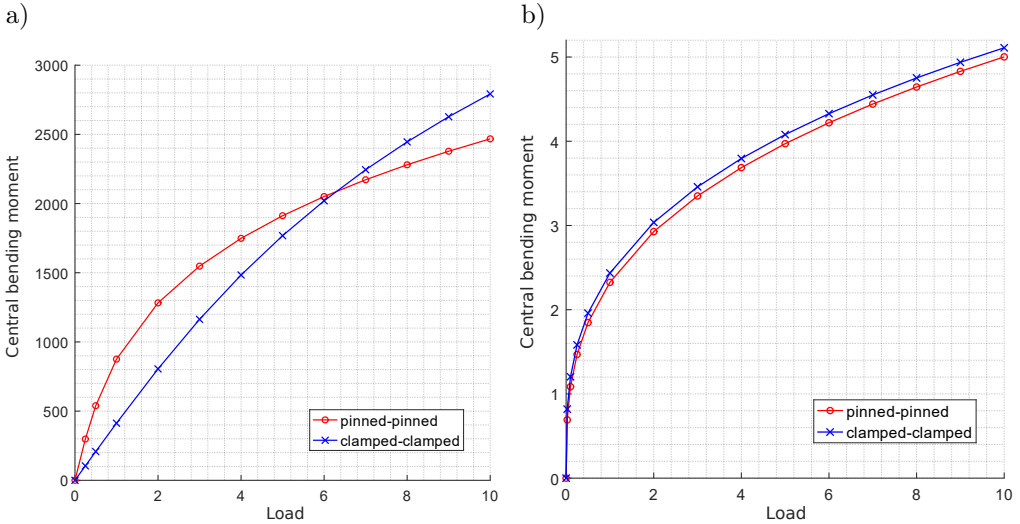


FIG. 11. Reference solution: central bending moment versus load for pinned-pinned and clamped-clamped beams with $L/d = 100$ (a) and $L/d = 1000$ (b).

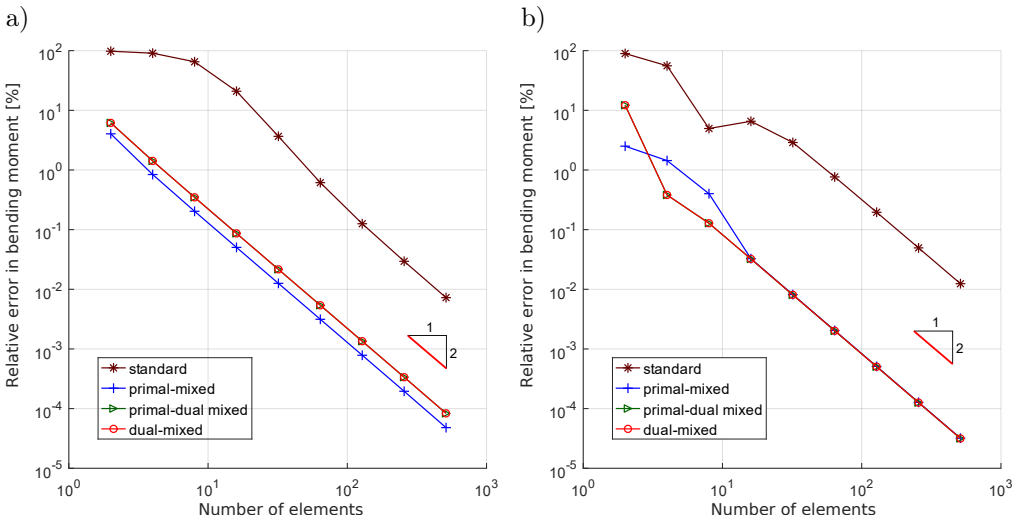


FIG. 12. Convergence of the relative error in bending moment at $x = L/2$ for the pinned-pinned beam with $L/d = 100$ (a) and $L/d = 1000$ (b) at the final load step $f_0 = 10$.

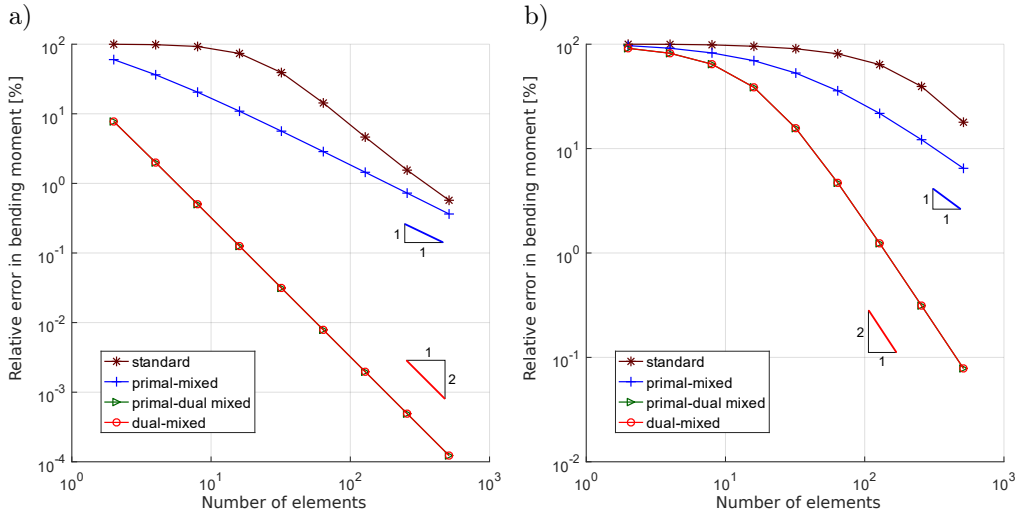


FIG. 13. Convergence of the relative error in bending moment at $x = L/2$ for clamped-clamped beam with $L/d = 100$ (a) and $L/d = 1000$ (b) at the final load step $f_0 = 10$.

convergence for the bending moment, independently of the boundary conditions applied. The standard and the primal-mixed elements give the first-order rate of asymptotic convergence for the clamped-clamped beam. The best choice for the bending moment computation, which is of primary interest in the design process of beam structures, is the dual-mixed or the primal-dual mixed element.

5. SUMMARY AND CONCLUSIONS

Analytical comparisons for the tangent stiffness matrices and the load vectors of four variational formulations, and the numerical performance of the related Galerkin-type finite element methods, have been presented for nonlinear shear-deformable beams, assuming von Kármán-type geometric nonlinearity. The finite element matrices of the standard displacement-based, a primal-mixed, a dual-mixed and a special primal-dual mixed formulation have been derived in their explicit forms by the computer algebra system MapleTM, using the lowest possible order of approximation spaces. To obtain comparable matrices for the dual-mixed and the primal-dual mixed elements, the λ -multiplier technique was applied.

The results of the direct comparisons of the element matrices showed that the coupling terms between the axial and the shear-bending deformations appeared only in the membrane part of the tangent stiffness matrices, the bending and shear parts remained unchanged during the incremental solution procedure. This means that the dual-mixed and the primal-dual mixed beam element operates with the exact bending and shear stiffness matrices of the linear beam element, independently of the slenderness of the beam.

The analytical investigations and explicit comparisons of the system matrices also show that the geometry-, material- and mesh-dependent constant C_s , given by Eq. (106), can be used to transform the tangent stiffness matrices of both the displacement-based and the primal-mixed beam element into the tangent stiffness matrix of the dual-mixed element, according to Eqs (103) and (113). The constant $1 \leq C_s < \infty$ can also be used as a shear locking indicator for the standard beam element: the higher the value of C_s , the more serious the shear locking is for the displacement-based element, and only $C_s = 1$ would indicate absolutely locking-free behavior, which can, theoretically, never be reached.

The performance of the four finite element models considered has been compared to each other through the numerical solutions of two simple model problems. As no analytic solutions for the nonlinear beam problems exist, high precision numerical solutions are computed for the displacements and the rarely listed stress variables as well, using the dual-mixed elements on an extremely refined mesh. These reference solutions are used for the numerical comparisons of the elements. The numerical results have been presented and compared not only for the deflections but also for the axial and shear forces, as well as the bending moments. It has been demonstrated that only the dual-mixed and the primal-dual mixed element gives the second-order rate of asymptotic convergence for the bending moment.

REFERENCES

1. F. Auricchio, B. Beirão da Veiga, J. Kiendl, C. Lovadina, A. Reali, Locking-free isogeometric collocation methods for spatial Timoshenko rods, *Computer Methods in Applied Mechanics and Engineering*, **263**: 113–126, 2013, doi: 10.1016/j.cma.2013.03.009.
2. K.-J. Bathe, *Finite element procedures*, Prentice-Hall, Upper Saddle River, New Jersey, 1996.
3. K.-J. Bathe, E.N. Dvorkin, A formulation of general shell elements – the use of mixed interpolation of tensorial components, *International Journal for Numerical Methods in Engineering*, **22**(3): 697–722, 1986, doi: 10.1002/nme.1620220312.
4. E. Bertóti, A comparison of primal- and dual-mixed finite element formulations for Timoshenko beams, *Engineering with Computers*, **31**: 99–111, 2015, doi: 10.1007/s00366-013-0333-y.
5. M. Bishoff, W.A. Wall, K.-U. Bletzinger, E. Ramm, Models and finite elements for thin walled structures, [in:] E. Stein, R. de Borst, T.J.R. Hughes [Eds], *The Encyclopedia of Computational Mechanics Vol. II*, pp. 59–137, John Wiley & Sons, New York, 2004.
6. D. Boffi, F. Brezzi, M. Fortin, *Mixed and hybrid finite element methods and applications*, Springer-Verlag, New York, 2013.
7. D. Chapelle, K.-J. Bathe, *The finite element analysis of shells – Fundamentals*. Springer-Verlag, Berlin, 2nd edition, 2011.

8. M. Géradin, A. Cardona, *Flexible multibody dynamics. A finite element approach*, John Wiley & Sons, Chichester, England, 2001.
9. T.J.R. Hughes, *The finite element method: Linear static and dynamic finite element analysis*, Prentice-Hall, Englewood Cliffs, New Jersey, 1987.
10. M. Igelbüscher, A. Schwarz, K. Steeger, J. Schröder, Modified mixed least-squares finite element formulations for small and finite strain plasticity, *International Journal for Numerical Methods in Engineering*, **117**(1): 141–160, 2018, doi: 10.1002/nme.5951.
11. W. Kim, J.N. Reddy, A comparative study of least-squares and the weak-form Galerkin finite element models for the nonlinear analysis of Timoshenko beams, *Journal of Solid Mechanics*, **2**(2): 101–114, 2010.
12. O. Klaas, J. Schröder, E. Stein, C. Miehe, A regularized dual mixed element for plane elasticity. Implementation and performance of the BDM element, *Computer Methods in Applied Mechanics and Engineering*, **121**(1–4): 201–209, 1995, doi: 10.1016/0045-7825(94)00701-N.
13. Y. Ko, Y. Lee, P.-S. Lee, K.-J. Bathe, Performance of the MITC3+ and MITC4+ shell elements in widely-used benchmark problems, *Computers and Structures*, **193**: 187–206, 2017, doi: 10.1016/j.compstruc.2017.08.003.
14. E. Marino, Locking-free isogeometric collocation formulation for three-dimensional geometrically exact shear-deformable beams with arbitrary initial curvature, *Computer Methods in Applied Mechanics and Engineering*, **324**: 546–572, 2017, doi: 10.1016/j.cma.2017.06.031.
15. C. Meier, A. Popp, W.A. Wall, Geometrically exact finite element formulations for slender beams: Kirchhoff-Love theory versus Simo-Reissner theory, *Archives of Computational Methods in Engineering*, **26**: 163–243, 2019, doi: 10.1007/s11831-017-9232-5.
16. A.K. Noor, J.M. Peters, Mixed models and reduced/selective integration displacement models for nonlinear analysis of curved beams, *International Journal for Numerical Methods in Engineering*, **17**(4): 615–631, 1981, doi: 10.1002/nme.1620170409.
17. J.P. Pontaza, Least-squares variational principles and the finite element method: theory, formulations, and models for solid and fluid mechanics, *Finite Elements in Analysis and Design*, **41**(7–8): 703–728, 2005, doi: 10.1016/j.finel.2004.09.002.
18. E.F. Punch, S.N. Atluri, Large displacement analysis of plates by a stress-based finite element approach, *Computers and Structures*, **24**(1): 107–117, 1986, doi: 10.1016/0045-7949(86)90339-1.
19. J.N. Reddy, On locking-free shear deformable beam finite elements, *Computer Methods in Applied Mechanics and Engineering*, **149**(1–4): 113–132, 1997, doi: 10.1016/S0045-7825(97)00075-3.
20. J.N. Reddy, *Energy principles and variational methods in applied mechanics*, John Wiley & Sons, New York, 2nd edition, 2002.
21. J.N. Reddy, *An introduction to nonlinear finite element analysis*, Oxford University Press, Oxford, UK, 2004.
22. J.E. Roberts, J.-M. Thomas, Mixed and hybrid methods, [in:] P.G. Ciarlet, J.L. Lions [Eds], *Handbook of Numerical Analysis*, Vol. II, pp. 523–639 North-Holland, Amsterdam, 1991.

23. J.C. Simo, T.J.R. Hughes, On the variational foundations of assumed strain methods, *Journal of Applied Mechanics*, **53**(1): 51–54, 1986, doi: 10.1115/1.3171737.
24. E. Stein, R. Rolfes, Mechanical conditions for stability and optimal convergence of mixed finite elements for linear plane elasticity, *Computer Methods in Applied Mechanics and Engineering*, **84**(1): 77–95, 1990, doi: 10.1016/0045-7825(90)90090-9.
25. B. Tóth, Hybridized dual-mixed hp -finite element model for shells of revolution, *Computers & Structures*, **218**: 123–151, 2019, doi: 10.1016/j.compstruc.2019.03.003.
26. K. Wiśniewski, *Finite rotation shells: Basic equations and finite elements for Reissner kinematics. Lecture notes on numerical methods in engineering and sciences*, CIMNE-Springer, Dordrecht, 2010.

Received July 6, 2020; revised version November 2, 2020.